Early Familial Dilated Cardiomyopathy: Identification with Determination of Disease State Parameter from Cine MR Image Data[1]

Juha R. Koikkalainen, DSc
Margareta Antila, MD
Jyrki M. P. Lötjönen, DSc
Tiina Heliö, MD
Kirsi Lauerma, MD
Sari M. Kivistö, MD
Petri Sipola, MD
Maija A. Kaartinen, MD
Satu T. J. Kärkkäinen, MD
Eeva Reissell, MD
Johanna Kuusisto, MD
Markku Laakso, MD
Matej Orešič, PhD
Markku S. Nieminen, MD
Keijo J. Peuhkurinen, MD

Purpose: To characterize early changes in cardiac anatomy and function for lamin A/C gene (*LMNA*) mutation carriers by using magnetic resonance (MR) imaging and to develop tools to analyze and visualize the findings.

Materials and Methods: The ethical review board of the institution approved the study, and informed written consent was obtained. The patient group consisted of 12 subjects, seven women (mean age, 36 years; age range, 18–54 years) and five men (mean age, 28 years; age range, 18–39 years) of Finnish origin, who were each heterozygotes with one *LMNA* mutation that may cause familial dilated cardiomyopathy (DCM). All the subjects were judged to be healthy with transthoracic echocardiography. The control group consisted of 14 healthy subjects, 11 women (mean age, 41 years; range, 23–54 years) and three men (mean age, 45 years; range, 34–57 years), of Finnish origin. Cine steady state free precession MR imaging was performed with a 1.5-T system. The volumes, wall thickness, and wall motion of both left ventricle (LV) and right ventricle were assessed. A method combining multiple MR image parameters was used to generate a global cardiac function index, the disease state parameter (DSP). A visual fingerprint was generated to assess the severity of familial DCM.

Results: The mean DSP of the patient group (0.69 ± 0.15 [standard deviation]) was significantly higher than that of the control group (0.32 ± 0.13) (P = .00002). One subject had an enlarged LV.

Conclusion: Subclinical familial DCM was identified by determination of the DSP with MR imaging, and this method might be used to recognize familial DCM at an early stage.

Supplemental material: *http://radiology.rsnajnls.org/cgi/content/full/249/1/88/DC1*
http://radiology.rsnajnls.org/cgi/content/full/249/1/88/DC2

[1] From the VTT Technical Research Centre of Finland, Tekniikankatu 1, FIN-33101 Tampere, Finland (J.R.K., J.M.P.L.); Helsinki Medical Imaging Center (M.A., K.L., S.M.K.) and Department of Cardiology (T.H., M.A.K., E.R., M.S.N.), Helsinki University Central Hospital, Helsinki, Finland; Departments of Radiology (P.S.) and Medicine (S.T.J.K., J.K., M.L., K.J.P.), Kuopio University Hospital, Kuopio, Finland; and VTT Technical Research Centre of Finland, Espoo, Finland (M.O.). Received September 7, 2007; revision requested November 13; revision received January 15, 2008; accepted March 28; final version accepted April 21. Supported by the Finnish Foundation for Cardiovascular Research, Medicine Fund of Helsinki University, Instrumentarium Foundation, Helsinki University Central Hospital Research Funds (EVO grants T1010K0002, TYH4241, and TYH7106), Finnish Foundation for Cardiovascular Research, and Finnish Funding Agency for Technology and Innovation. **Address correspondence to** J.R.K. (e-mail: *juha.koikkalainen@vtt.fi*).

Dilated cardiomyopathy (DCM) is characterized by enlargement and impaired contraction of the left ventricle (LV) or both LV and right ventricle (RV) (1,2). One-third to one-half of the cases of DCM are familial (3). With an estimated prevalence of 36 in 100 000 adults in the United States (4), DCM is an important cause of heart failure and the leading cause for heart transplantation (5,6). During the past years, several genetic factors of DCM have been identified (7–9). So far, the most important gene in the risk for cardiomyopathy is the lamin A/C gene (*LMNA*) (10–13), which codes for a structural protein of the nuclear envelope (14). *LMNA* mutations are associated with serious cardiomyopathy with conduction defects, ventricular arrhythmias, and sudden death by middle age (10–13,15–17). Moreover, in a recent study, 9% of patients with cardiac transplantation proved to be heterozygotes with an *LMNA* mutation (6). Because the ventricular dilatation in patients with cardiomyopathy related to *LMNA* mutations may be modest (12), recognition of the disease at an early stage is difficult.

Echocardiography is regarded as the standard method to clinically study DCM. However, volumetric measurements are difficult to determine because of the low apical visibility (18). Echocardiography is highly dependent on the physician's experience, and in some patients, the visibility is suboptimal (18). MR imaging has proved to be more reliable than echocardiography in measuring LV volume, mass, and ejection fraction (19–21) and wall thickness (21).

Advances in Knowledge

- A computational disease state parameter (DSP) constructed from MR image parameters summarizes multiple early changes in cardiac anatomy and function in carriers of lamin A/C mutations.
- The mean DSP of the patient group (0.69 ± 0.15) was significantly higher than that of the control group (0.32 ± 0.13) ($P = .00002$).

Each cine MR imaging session produces a large amount of data, and in clinical practice only a fraction of the obtainable parameters are used for diagnosis. Although segmentation tools are already commercially available, the analysis of multiple volumetric and wall motion parameters requires manual work and depends on the clinical skills of the radiologist or cardiologist.

We hypothesized that cardiac cine MR imaging can be used to produce accurate parameters to recognize familial DCM at an early stage. Therefore, the purpose of the study was to characterize the early changes in cardiac anatomy and function for *LMNA* mutation carriers by using MR imaging and to develop tools to analyze and visualize the findings.

Materials and Methods

VTT is an impartial expert organization under the Ministry of Trade and Industry (Finland). VTT has filed a patent application on the data analysis and visualization methods presented in this article and has interest to exploit this patent and related software tool by licensing.

The ethical review board of Helsinki University Central Hospital, Helsinki, Finland approved the study, and informed written consent was obtained from the participants. MR imaging studies were performed between 2002 and 2006.

Study Population

The clinical characteristics and electrocardiographic and echocardiographic findings in the patients are shown in Table 1. The patient group comprised 12 subjects, seven women (mean age, 36 years ± 13 [standard deviation]; range, 18–54 years) and five men (mean age, 28 years ± 8; range, 18–39 years), of Finnish origin who were heterozygotes with one *LMNA* mutation. These subjects belonged to nine families. The original probands of the families with DCM had belonged to either of the following study groups: *(a)* Finnish DCM patients who had received a heart transplant between 1984 and 1998 (6), or *(b)* 20 well-characterized patients with familial DCM and 70 sporadic DCM patients from the Kuopio University Hospital region in Eastern Finland and the Helsinki University Hospital region (12) in Finland. To establish a diagnosis in these probands, commonly approved diagnostic criteria (LV ejection fraction < 45% and surface area–normalized LV ED diameter > 27 mm/m^2 at echocardiography at the time of diagnosis) were applied, and all secondary causes of DCM (1) were carefully excluded. The participants did not have any signs or symptoms of skeletal muscle disease, and the creatine kinase con-

Implications for Patient Care

- Cardiac MR imaging could be a tool for early diagnosis of familial dilated cardiomyopathy (DCM) to help the physician to decide which patients need a close follow-up to use the possible pharmacologic, device, or surgical therapy in a timely manner.
- Minor changes at cardiac MR imaging that indicate early familial DCM could be an indicator for genetic counseling and risk stratification in the patient.

Published online
10.1148/radiol.2491071584

Radiology 2008; 249:88–96

Abbreviations:
DCM = dilated cardiomyopathy
DSP = disease state parameter
ED = end diastole
ES = end systole
LV = left ventricle
RV = right ventricle
SMM = statistical motion model

Author contributions:
Guarantors of integrity of entire study, J.R.K., M.A., K.L., K.J.P.; study concepts/study design or data acquisition or data analysis/interpretation, all authors; manuscript drafting or manuscript revision for important intellectual content, all authors; manuscript final version approval, all authors; literature research, J.R.K., M.A., J.M.P.L., T.H., K.L., P.S., S.T.J.K., K.J.P.; clinical studies, M.A., T.H., K.L., S.M.K., M.A.K., S.T.J.K., E.R., J.K., M.S.N., K.J.P.; experimental studies, J.R.K., M.A., J.M.P.L., M.L.; statistical analysis, J.R.K., J.M.P.L.; and manuscript editing, J.R.K., M.A., J.M.P.L., T.H., K.L., S.M.K., P.S., M.A.K., S.T.J.K., J.K., M.O., M.S.N., K.J.P.

See Materials and Methods for pertinent disclosures.

centration was normal. From these families, all available New York Heart Association class I *LMNA* mutation carriers with echocardiographic findings that did not fulfill the DCM criteria were included in this analysis.

The control group consisted of 14 healthy subjects, 11 women (mean age, 41 years ± 12; range, 23–54 years) and three men (mean age, 45 years ± 12; range, 34–57 years), who did not have any cardiac risk factors or family history of cardiac disease, a history of diabetes, coronary artery disease, or valvular or hypertensive disease. None of them was taking any medication known to influence cardiac function. Electrocardiographic data were normal in all subjects. There were no significant differences in the age distributions of the patient and control groups.

Evaluation Methods

The patients were evaluated by using personal and family history; physical examination; 12-lead electrocardiogram; and M-mode, two-dimensional, and Doppler transthoracic echocardiography (Vivid 7; GE Medical Systems, Horten, Norway). The echocardiographic examinations were performed by experienced cardiologists (T.H., M.A.K., E.R., with 8–10 years of experience each). In all subjects, results of transthoracic echocardiography indicated that the patients were healthy.

Cine MR imaging was performed with a 1.5-T system (Sonata; Siemens Medical Solutions, Erlangen, Germany) and a body-array coil. A retrospectively electrocardiographically gated segmented steady-state free precession imaging sequence was used with the following parameters: repetition time msec/echo time msec, 3.0/1.6; matrix, 256 × 256; field of view, 240 × 340 mm; and flip angle, 52°. A short-axis cine stack and a long-axis cine section of both ventricles were obtained, with a section thickness of 6 mm, an intersection gap of 20%, and a temporal resolution of 42–49 msec. Examples of the cine MR imaging series are shown in Movies 1–4 (*http://radiology.rsnajnls.org/cgi/content/full/249/1/88/DC2*).

The LV, RV, and epicardium were semiautomatically segmented by a tech-

Table 1

Clinical Characteristics and Electrocardiographic and Echocardiographic Findings in 12 Heterozygous *LMNA* Mutation Carriers

Characteristic	Mutation Carriers	*P* Value*
Sex		
Men		
No. of patients	5	.401
Age (y)	28 ± 8 (18–39)	.071
Women		
No. of patients	7	.401
Age (y)	36 ± 13 (18–54)	.596
Body mass index for men and women (kg/m^2)	24 ± 4	.494
LMNA mutation heterozygotes†		
No. with Ser143Pro	8	<.001
No. with Thr1085del	1	.462
No. with Ala132Pro	2	.203
No. with Arg190Trp	1	.462
Cardiac symptoms		
No. with New York Heart Association class I	12	>.99
No. with dyspnea	2	.203
No. with atypical chest pain	1	.462
No. with presyncope and syncope	0	>.99
No. with palpitation	5	.012
No. with paroxysmal atrial flutter	1	.462
12-Lead electrocardiographic results		
No. with sinus rhythm	12	>.99
No. with LV hypertrophy	1	.462
No. with intraventricular conduction defect	1	.462
No. with first-degree atrioventricular block	6	.004
No. with pathologic Q wave	1	.462
No. with ventricular extrasystole	1	.462
Echocardiographic results		
LV ED diameter (mm)	50 ± 4	. . .
Ejection fraction (%)	63 ± 7	. . .
Left atrial diameter (mm)	33 ± 6	. . .
E/A ratio	1.7 ± 0.4	. . .
No. with mitral regurgitation	0	. . .
No. with increased brain natriuretic peptide propeptide concentration	1	. . .
Medications		
No. receiving a beta-blocker‡	1	.462
No. receiving warfarin§	1	.462
No. receiving levothyroxine‖	1	.462
No. receiving a contraceptive#	1	.462

Note.—Data are the mean ± standard deviation except where otherwise indicated. Numbers in parentheses are ranges. E/A ratio = peak mitral early diastolic and atrial contraction velocity ratio, ED = end diastolic.

* Compared with control subjects.

† Ser143Pro = serine at residue 143 replaced by proline, Thr1085del = threonine deleted at position 1085, Ala132Pro = alanine at residue 132 replaced by proline, and Arg190Trp = arginine at residue 190 replaced by tryptophan.

‡ The beta-blocker was bisoprolol (Emconcor CHF; Merck, Darmstadt, Germany).

§ Warfarin sodium, Marevan; Orion Pharma, Turku, Finland.

‖ Levothyroxine sodium, Thyroxin; Orion Pharma.

The contraceptive was 30 μg ethinylestradiol and 0.15 mg levonorgestrel (Microgynon; Bayer Schering Pharma, Turku, Finland.

nician (J.M.P.L., with 10 years of experience), together with a radiologist (K.L., with 10 years of experience), from each time frame of the cine MR image series with a software tool developed for this purpose (22). The automatic segmentation took 1–2 minutes. To reach the optimal segmentation accuracy, the time used for the manual refinement was not limited, and it took approximately 30 minutes. In the tool, an a priori heart model, consisting of triangular surfaces of the LV, RV, and epicardium, was deformed to fit both short- and long-axis MR image data. Because the same a priori model was used for each subject, the number of the surface points was identical in each case, and point correspondence existed between all the subjects and the time frames. The surfaces were rigidly aligned in the same coordinate system to remove the position and orientation variations from the data. This enabled pointwise comparison of the cardiac motion in the study population.

Table 2

Measurements Determined from Imaging Data

Measurement	Description
Volumetric data	
$EDV_{LV/RV}$	ED volume of LV divided by surface area or RV divided by surface area
$ESV_{LV/RV}$	ES volume of LV divided by surface area or RV divided by surface area
$SV_{LV/RV}$	Stroke volume of LV divided by surface area or RV divided by surface area
$EF_{LV/RV}$	Ejection fraction of LV or RV
$PER_{LV/RV}$	Peak ejection rate of LV or RV
$TPER_{LV/RV}$	Time to peak ejection rate of LV or RV
$PFR_{LV/RV}$	Peak filling rate of LV or RV
$TPFR_{LV/RV}$	Time to peak filling rate of LV or RV
Wall thickness data	
EDT_{LVN}	ED thickness of LV wall of *N*th segment
EDT_{LVg}	ED thickness of whole LV wall
Wall thickening data	
Th_{LVN}	Relative wall thickening of LV wall of *N*th segment
Th_{LVg}	Relative wall thickening of whole LV wall
Wall motion data	
$WM_{LVN/RVN}$	Norm of motion of LV wall of *N*th segment or RV wall of *N*th segment
$WM_{LVg/RVg}$	Norm of motion of whole LV wall or RV wall
$SMMmn_{LV/RV}$*	Mean of absolute values of weights of SMM of LV or RV
$SMMmx_{LV/RV}$*	Maximum of absolute values of weights of SMM of LV or RV
$SMMrs_{LV/RV}$*	Residual error of SMM approximation of LV or RV

* SMM = statistical motion model. The SMM is explained in reference 23.

Figure 1

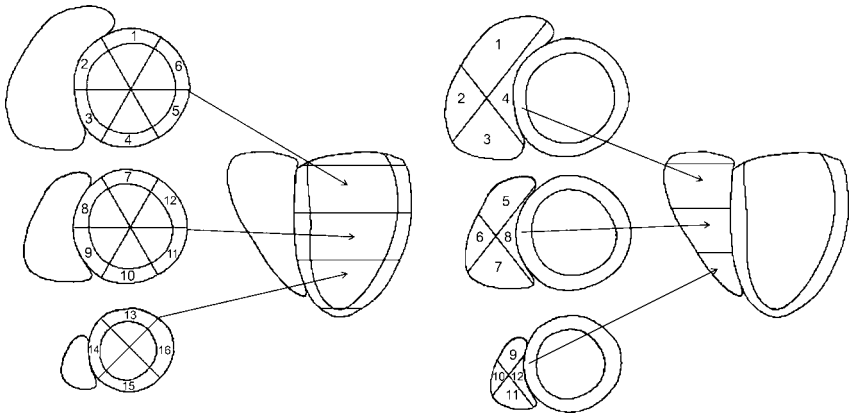

Figure 1: Segmental division of LV (16 segments) and RV (12 segments) (24). Most basal and apical levels were not included in segments.

Image Quantification

In total, 86 measurements were determined from the MR image data. Four types of measurements were used: *(a)* volumetric measurements, *(b)* LV wall ED thickness, *(c)* LV wall thickening from ED to end systole (ES), and *(d)* measurements describing the motion of the LV and RV (Table 2). The measurements were determined globally. In addition, wall thickness, wall thickening, and wall motion measurements were derived on a per-segment level (Fig 1).

The wall motion measurement was determined as follows. The distance from the wall of the ventricle to the midpoint of the ventricle was computed both at ED as d_{ED} and at ES as d_{ES}. The midpoints of the LV and RV were determined for each short-axis plane of the segmental model. The wall motion measurement, WM, was then computed as $WM = d_{ED} - d_{ES}$.

An SMM (23) was constructed from the motion of the center points of the wall segments. In SMM, the principal component analysis was applied to the variations in the data, which yielded a set of modes of variation that described the typical motion patterns in the data. Weights corresponding to each mode of variation were computed for the motion data of each subject. The SMM can explain exactly only the motion of the subjects used to build the model, and modeling errors appear for unseen subjects. In this work, the SMM was built from the control subjects. Three measurements were computed to study how accurately the motion of the patients resembled the motion of the control sub-

Figure 2

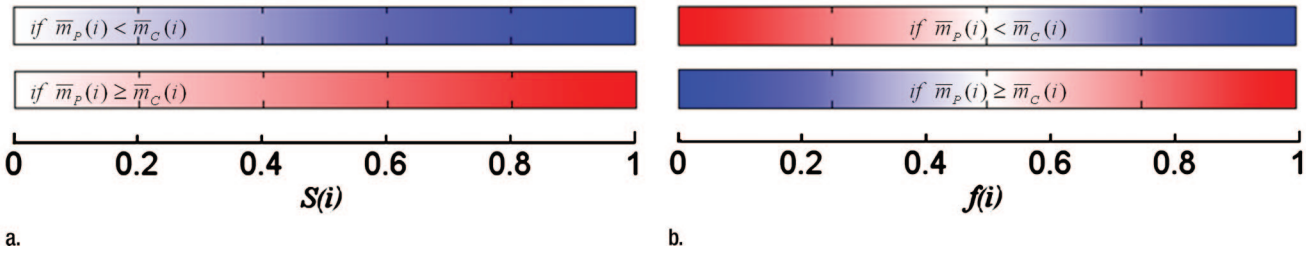

Figure 2: Color coding used in fingerprint visualizations for **(a)** group-to-group and **(b)** subject-to-group comparisons. **(a)** Colors were dependent on significance value $S(i)$ of measurement. **(b)** Colors were determined on basis of fitness value $f(i)$ of the measurement. Different mapping of colors was used for cases $\bar{m}_P(i) < \bar{m}_C(i)$ and $\bar{m}_P(i) \geq \bar{m}_C(i)$ to visualize sign of difference from mean of control group, where $\bar{m}_P(i)$ and $\bar{m}_C(i)$ were mean measurement values of patient and control groups, respectively.

jects: the mean and maximum of the absolute values of the weights and the magnitude of the modeling error.

Significance Values for Measurements

The nonparametric Wilcoxon rank sum test (25) was performed for each measurement to determine which measurements had significantly different values in control and patient groups. A significance value of the ith measurement, $S(i)$, was computed from the P values, $P(i)$, obtained from the statistical tests by mapping the values to an easily understandable range of 0–1 (Appendix E1 [*http://radiology.rsnajnls.org/cgi/content/full/249/1/88/DC1*]), where the value $S(i) = 0$ meant that there was no difference between the groups and the value $S(i) = 1$ meant that the difference was significant.

Comparison of Subject Data with Group Data

Next, we studied how the measurement values of a target subject fit to the distributions of the corresponding measurements in the control and patient groups. The probabilities $P_P(i)$ and $P_C(i)$ were determined to estimate the likelihood that the ith measurement came from a patient, $P_P(i)$, or control subject, $P_C(i)$ (Appendix E1 [*http://radiology.rsnajnls.org/cgi/content/full/249/1/88/DC1*]). The fitness value of the ith measurement was obtained from the following equation: $f(i) = P_P(i)/[P_P(i) + P_C(i)]$. This value measured how well the ith measurement value fit to the distributions of both the control and patient groups. This equation was selected to yield a reasonable range of 0–1 for the fitness values: Thus, $f(i) = 0$ meant that the measurement was completely different from the patient group values, $f(i) = 1$ meant that the measurement was completely different from the control group values, and $f(i) = 0.5$ meant that it was equally probable that the measurement arose from a subject with disease as from a healthy subject.

Finally, a disease state parameter (DSP), a global assessment parameter of ventricular function, of the target subject was computed by combining the fitness values of all the measurements.

Table 3

Volumetric Cine MR Imaging Results in Patients and Control Subjects

Clinical Data and MR Measurements	Patients	Control Subjects	*P* Value
Clinical data			
No. of patients	12	14	
Sex			
Women			
No. of patients	7	11	.401
Age (y)	36 ± 13	41 ± 12	.596
Men			
No. of patients	5	3	.401
Age (y)	28 ± 8	45 ± 12	.071
Body mass index for women and men (kg/m^2)	24 ± 4	26 ± 6	.494
Surface area (m^2)	1.9 ± 0.3	1.8 ± 0.2	.494
MR measurements			
LV volume divided by surface area			
ED volume (mL/m^2)	93 ± 13	80 ± 20	.031
ES volume (mL/m^2)	36 ± 7	24 ± 7	.0009
LV function			
Stroke volume (mL/m^2)	57 ± 10	56 ± 13	.494
Ejection fraction (%)	61 ± 6	70 ± 3	.00002
RV volume divided by surface area			
ED volume (mL/m^2)	91 ± 21	76 ± 21	.076
ES volume (mL/m^2)	37 ± 10	32 ± 11	.118
RV function			
Sroke volume (mL/m^2)	53 ± 14	44 ± 11	.085
Ejection fraction (%)	59 ± 5	58 ± 3	.86

Note.—Data are the mean ± standard deviation except where otherwise indicated.

As the significance value $S(i)$ estimated how much discriminative information the ith measurement contained, it was reasonable to give more weight to the measurements that had a large $S(i)$, as expressed thus:

$$\mathrm{DSP} = \frac{\sum_i S(i)f(i)}{\sum_i S(i)}.$$

The value of the DSP described how closely the measurement values, and, therefore, the ventricular function, of the target subject matched with the corresponding values in the patient group. Values close to one were indications of a severe state of disease, and healthy subjects should have had values close to zero. Therefore, DSP was used to quantitatively analyze the overall situation of the cardiac function in the target subject.

Fingerprint Visualization

In addition to the automatic quantitative analysis, a visualization tool was developed to enable qualitative visual analysis of both the subject-to-group and group-to-group differences. Differences in the data were highlighted by using color codes. In the group-to-group comparison, the colors were obtained from the significance value $S(i)$ (Fig 2a). In the subject-to-group comparison, the colors were based on the fitness value $f(i)$ (Fig 2b). The exact mathematic definitions of the color coding are provided in Appendix E1 (*http://radiology.rsnajnls.org/cgi/content/full/249/1/88/DC1*). Group-to-group visualization gave a fingerprint of a disease when compared with the control group. Similarly, subject-to-group visualization provided a fingerprint for a subject. Because the color codes of the group-to-group and subject-to-group analyses were comparable, the visualizations could be used to study how well the subject fit to the patient group by comparing the fingerprints of the disease and the subject.

Leave-One-Out Cross Validation

To eliminate the risk of overfitting the model, the study was performed by using full leave-one-out cross validation. One subject (patient or control subject) was removed from the study population, and the DSP value and the fingerprint visualization were computed for this subject. Consequently, the data in the target subject were not used in the training of the model. This was repeated for each subject.

Figure 3

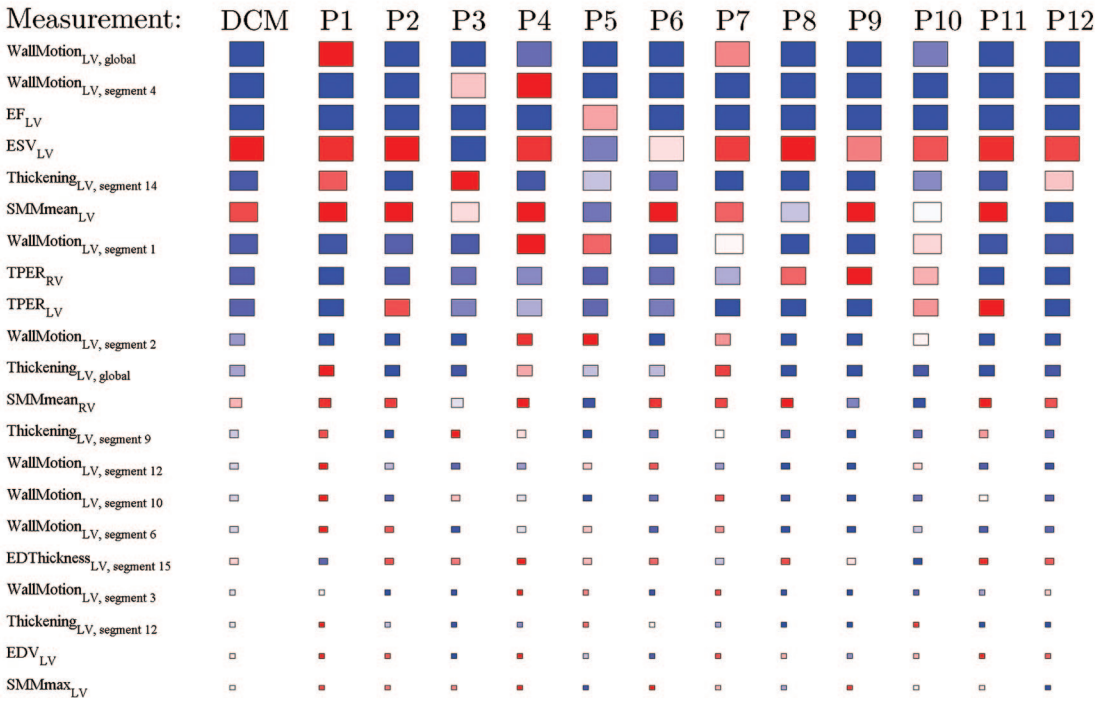

Figure 3: Fingerprints for whole disease (DCM) group and for all patients *(P1–P12).* In group-to-group comparison (DCM), red (blue) shows that mean measurement of patient group was larger (smaller) than mean measurement of control group. The darker the color was, the more significant the differences between the control and patient groups were. In subject-to-group comparison *(P1–P12),* if fitness value *f (i)* had large positive value and mean value of patient group was larger than mean value of patient group, dark red was used. If mean value of patient group was smaller than mean value of patient group, dark blue was used. If fitness value was negative (ie, measurement value did not fit to distribution of measurement values in patient group), blue (red) was used. Size of box was in proportion to significance value *S (i)* of measurement (the more reliable the measurement was, the larger the box). Measurements were ordered on basis of significance value, and only measurements with significance value larger than zero are shown. To enable compact presentation where same DCM fingerprint was used for each subject, significance values *S (i)* were not computed by using cross validation. *EDV* = ED volume, *EF* = ejection fraction, *ESV* = ES volume, *TPER* = time to peak ejection rate.

Figure 4

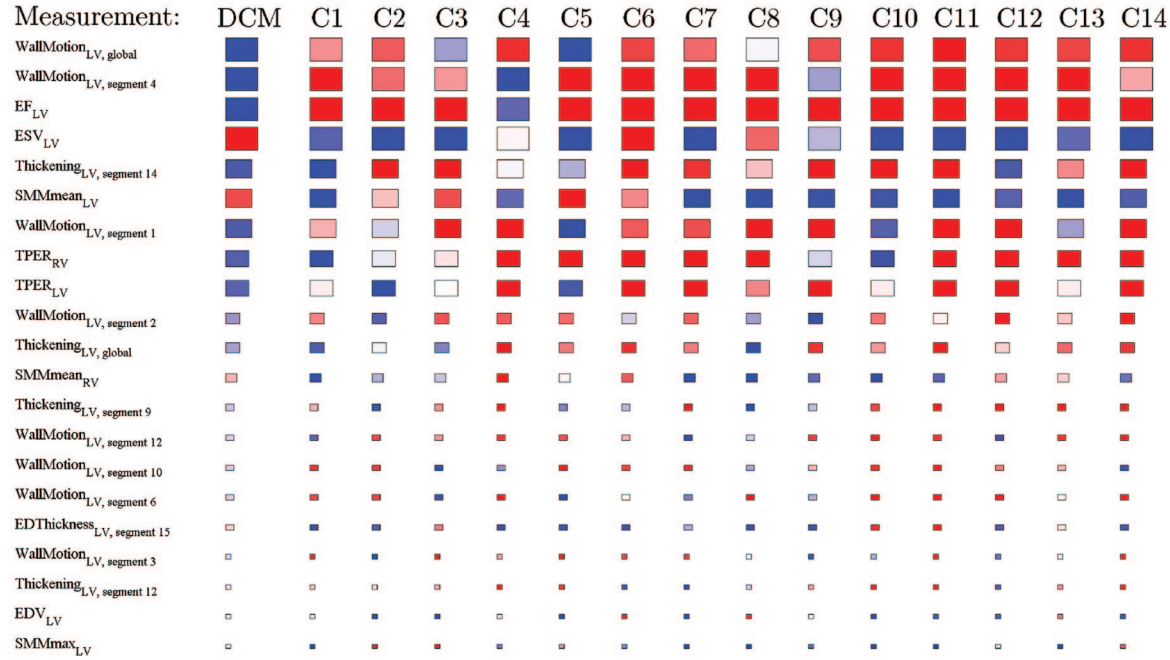

Figure 4: Fingerprints for whole disease (DCM) group and for all control subjects *(C1–C14)*. Details and keys are same as in Figure 3.

After the segmentation of the target data was available, the computations took less than 10 seconds. The analyses were computed, and visualizations were generated by using software (Matlab R2006a, version 7.2; MathWorks, Natick, Mass).

Statistical Analysis

The statistical analyses of the continuous data (such as DSP, measurements, and age) were performed by using the Wilcoxon rank sum (Mann-Whitney) test (25), and the Fisher exact test (26) was used for dichotomous data (such as sex and symptoms). Other software (SPSS for Windows, release 14.0.1; SPSS, Chicago, Ill) was used to perform the statistical tests. A *P* value of less than .05 was considered to represent a significant difference.

Results

All the patients belonged to New York Heart Association functional class I (Table 1). Five patients were asymptomatic, and the most common symptom was palpitation. All patients had sinus rhythm during MR imaging, and half of them showed first-degree atrioventricular block on the electrocardiogram. Only one patient had marginally increased serum brain natriuretic peptide propeptide concentration. One patient was using a beta-blocker and warfarin sodium for paroxysmal atrial flutter.

On the basis of the current guidelines (27,28) for echocardiography, in none of the subjects in our patient group was a diagnosis of DCM established. All patients had a normal LV ejection fraction (range, 52%–73%), and only one patient had an enlarged LV (range of percentage of predicted value of LV ED dimension corrected for age and surface area [29], 93%–118%). LV ED and LV ES volumes divided by surface area were significantly greater in patients than in control subjects (Table 3). LV ejection fraction was significantly lower in patients; the smallest value was 49%. There were no significant dependencies among age, sex, or age multiplied by sex and the measurements reported.

There is a good overall similarity between the fingerprint of DCM and the fingerprints of the 12 patients whose data are shown on Figure 3. On the other hand, the fingerprints of the control subjects largely differ from the fingerprint of DCM (Fig 4). No single measurement gives perfect discrimination between the patients and control subjects, but by examining the entire fingerprint, the differences are evident. The mean DSP of the patient group (0.69 ± 0.15) was significantly higher than that of the control group (0.32 ± 0.13) ($P = .00002$) (Fig 5).

Discussion

This study introduces an MR image–based method for estimation of the disease state in patients with familial DCM caused by *LMNA* mutations. Functional parameters that change in these mutations were identified, and their weighted combination was used to calculate a DSP for each study subject. The DSP of the *LMNA* mutation carriers with normal findings at transthoracic echocardiography proved to be significantly different from that of the control group. We demonstrated visualization of the individual disease state in a comparison of healthy control subjects and familial DCM patients with an *LMNA* mutation.

A small but genetically verified group of patients was included in this study. We used a standard MR machine, coil, and cine MR imaging protocol to obtain the functional information in the subjects. A large set of measurements was determined with a software tool developed for this purpose (22). The simultaneous use of both short- and long-axis data facilitated the accurate quantification of the ventricular function, especially in basal and apical regions. Because single measurements could not be used to reliably differentiate the patients from the control subjects, the combination of weighted parameters was developed. The use of MR imaging enabled quantification of a large set of measurements that were not obtained by using echocardiography.

Our patients had an early state of familial DCM. Five of 12 patients were asymptomatic, although six of them had atrioventricular block. At echocardiography, one patient had an enlarged LV but otherwise the echocardiographic findings were normal. At MR imaging, a significant increase in LV ED and LV ES volumes divided by surface area and a decrease in ejection fraction were observed when these values were compared with those in control subjects. In spite of the relatively asymptomatic state of the disease, a significant difference was observed between the study groups by combining the information from all 86 MR image parameters.

The fingerprint of DCM showed that the values for global motion and the motion of segment 4 of the LV wall were smaller in the patient group than in the control group. Similar results have been reported in a study (30) about familial DCM patients in which tagged MR images were used; considerable circumferential heterogeneity at the basal level and relatively normal lateral wall function were observed. The site of the wall motion abnormality is consistent with that in another report about late enhancement in the basal segments (31).

LMNA mutations are the most common genetic defects encountered in familial DCM (9,12). The *LMNA* carriers usually have a progressive disease that causes severe symptoms, sudden death, and the need for cardiac transplantation (12,13,15–17). Because of the malignant nature of the disease, the first-degree relatives should be screened for the specific mutation. However, the mutation carriers are often asymptomatic and have normal echocardiographic findings, as in the present series, or only mild dilatation or near-normal function of the LV. We showed that the DSP calculated from the cine MR image data can, however, be used to identify familial DCM patients at an early stage. The presented method could be easily applied for follow-up of patients, as well. At the moment, it is not definitively known when to start treatment with beta-blockers, angiotensin-converting–enzyme inhibitors, or angiotensin II receptor type 1 blocking agents in patients with relatively well preserved systolic function, but trials on this important issue are currently going on.

The approach described here could be used for phenotyping other genetic cardiomyopathies, such as hypertrophic cardiomyopathy, and for recognizing early cytotoxic cardiomyopathies. The method could also be useful for studying the mechanisms of LV remodeling in various heart diseases. The mathematic method presented in this article is not limited to the analysis of cine MR image data but can be used with other imaging modalities. Furthermore, the imaging parameters could be combined with parameters obtained from appropriate metabolic and genetic analyses. The current tool was developed for the analysis of cardiac diseases, but the concept can be adapted to other disease states.

A limitation in our study was that the study group was small. However, the *LMNA* mutations are relatively rare, and our *LMNA* mutation group was the largest described with MR imaging, to our knowledge. Patients with a more severe state of disease could have been included in the study, but atrial fibrillation and pacemakers are more common in these patients and would have hindered MR imaging. On the other hand, diagnoses in these subjects could have been established with echocardiography, and, therefore, including them in the study would not have supported objectives of this study. Another limitation was that the measurements correlated with each other, and an index determined by using a combination of such measurements contains redundancy. Therefore, the method used does not necessarily yield mathematically optimal efficiency (which would have been obtained when measurements were independent). However, mathematically optimal efficiency was not the goal of this study: It was considered more important to obtain an intuitively plausible index. One possible method to remove the correlations would be to apply the principal component analysis to the data, which would produce a set of uncorrelated measurements. However, these newer parameters would not be as intuitive as the original ones. Evaluation of the true clinical effect of the method requires large longitudinal validation studies with subjects from several patient groups. The specificity of the method was not studied either. Even if the method was capable of discrimination of the patients from the healthy control subjects, it is not known, for example, whether different types of cardiomyopathies could be differentiated from each other. It has to be noted in this context, however, that large clinical trials for testing the effects of beta-blockers, angiotensin-converting enzyme inhibitors, or angiotensin II receptor type 1 blockers, or all three, in patients with heart failure have shown benefits for all patients regardless of the cause of cardiac dysfunc-

Figure 5

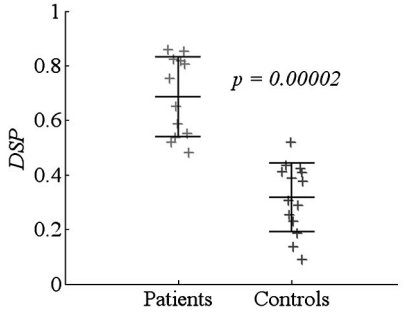

Figure 5: DSPs and their mean values and standard deviations for both patient and control groups. Differences between groups were analyzed by using Wilcoxon rank sum test.

tion (eg, ischemic vs nonischemic cardiomyopathy). Therefore, specificity in terms of treatment may not be a major issue.

To further develop and improve the method, an optimal set of measurements should be searched, which would lead to a set of uncorrelated or independent variables that are mathematically efficiently combined. The inter- and intraobserver variabilities of the assessment of the fingerprint visualization have to be evaluated and the optimal way of visualization determined. The required accuracy of the segmentation has to be estimated to optimize the time needed for the manual refinement of the segmentation.

In conclusion, a computational DSP constructed from MR image parameters is capable of being used for the detection of early cardiac changes that cannot be detected with conventional echocardiography in *LMNA* mutation carriers. In this study, a visualization tool that was introduced enables the visual analysis of the changes in the parameters. The method presented here could be tested in different patient populations and in future clinical trials.

Acknowledgments: MR imaging was performed by two radiographers, Timo Päivärinta and Aki Syrjälä. We thank Sini Weckström for excellent technical assistance and docent Mark van Gils for the assistance in finishing the manuscript. We thank the family members with DCM and healthy control subjects for their participation in our study.

References

1. Maron BJ, Towbin JA, Thiene G, et al. Contemporary definitions and classification of the cardiomyopathies: an American Heart Association Scientific Statement from the Council on Clinical Cardiology, Heart Failure and Transplantation Committee; Quality of Care and Outcomes Research and Functional Genomics and Translational Biology Interdisciplinary Working Groups; and Council on Epidemiology and Prevention. Circulation 2006;113:1807–1816.
2. Richardson P, McKenna W, Bristow M, et al. Report of the 1995 World Health Organization/International Society and Federation of Cardiology Task Force on the Definition and Classification of cardiomyopathies. Circulation 1996;93:841–842.
3. Grunig E, Tasman JA, Kucherer H, Franz W, Kubler W, Katus HA. Frequency and phenotypes of familial dilated cardiomyopathy. J Am Coll Cardiol 1998;31:186–194.
4. Codd MB, Sugrue DD, Gersh BJ, Melton LJ 3rd. Epidemiology of idiopathic dilated and hypertrophic cardiomyopathy: a population-based study in Olmsted County, Minnesota, 1975–1984. Circulation 1989;80:564–572.
5. Dec GW, Fuster V. Idiopathic dilated cardiomyopathy. N Engl J Med 1994;331:1564–1575.
6. Karkkainen S, Reissell E, Helio T, et al. Novel mutations in the lamin A/C gene in heart transplant recipients with end stage dilated cardiomyopathy. Heart 2006;92:524–526.
7. Fatkin D, Graham RM. Molecular mechanisms of inherited cardiomyopathies. Physiol Rev 2002;82:945–980.
8. Morita H, Seidman J, Seidman CE. Genetic causes of human heart failure. J Clin Invest 2005;115:518–526.
9. Karkkainen S, Peuhkurinen K. Genetics of dilated cardiomyopathy. Ann Med 2007;39:91–107.
10. Fatkin D, MacRae C, Sasaki T, et al. Missense mutations in the rod domain of the lamin A/C gene as causes of dilated cardiomyopathy and conduction-system disease. N Engl J Med 1999;341:1715–1724.
11. Arbustini E, Pilotto A, Repetto A, et al. Autosomal dominant dilated cardiomyopathy with atrioventricular block: a lamin A/C defect-related disease. J Am Coll Cardiol 2002;39:981–990.
12. Karkkainen S, Helio T, Miettinen R, et al. A novel mutation, Ser143Pro, in the lamin A/C gene is common in finnish patients with familial dilated cardiomyopathy. Eur Heart J 2004;25:885–893.
13. Hershberger RE, Hanson EL, Jakobs PM, et al. A novel lamin A/C mutation in a family with dilated cardiomyopathy, prominent conduction system disease, and need for permanent pacemaker implantation. Am Heart J 2002;144:1081–1086.
14. Hutchison CJ, Alvarez-Reyes M, Vaughan OA. Lamins in disease: why do ubiquitously expressed nuclear envelope proteins give rise to tissue-specific disease phenotypes? J Cell Sci 2001;114:9–19.
15. Jakobs PM, Hanson EL, Crispell KA, et al. Novel lamin A/C mutations in two families with dilated cardiomyopathy and conduction system disease. J Card Fail 2001;7:249–256.
16. Taylor MR, Fain PR, Sinagra G, et al. Natural history of dilated cardiomyopathy due to lamin A/C gene mutations. J Am Coll Cardiol 2003;41:771–780.
17. van Berlo JH, de Voogt WG, van der Kooi AJ, et al. Meta-analysis of clinical characteristics of 299 carriers of LMNA gene mutations: do lamin A/C mutations portend a high risk of sudden death? J Mol Med 2005;83:79–83.
18. Mulvagh SL, DeMaria AN, Feinstein SB, et al. Contrast echocardiography: current and future applications. American Society of Echocardiography Task Force on Standards and Guidelines for the Use of Ultrasonic Contrast in Echocardiography. J Am Soc Echocardiogr 2000;13:331–342.
19. Grothues F, Smith GC, Moon JC, et al. Comparison of interstudy reproducibility of cardiovascular magnetic resonance with two-dimensional echocardiography in normal subjects and in patients with heart failure or left ventricular hypertrophy. Am J Cardiol 2002;90:29–34.
20. Strohm O, Schulz-Menger J, Pilz B, Osterziel KJ, Dietz R, Friedrich MG. Measurement of left ventricular dimensions and function in patients with dilated cardiomyopathy. J Magn Reson Imaging 2001;13:367–371.
21. Pujadas S, Reddy GP, Weber O, Lee JJ, Higgins CB. MR imaging assessment of cardiac function. J Magn Reson Imaging 2004;19:789–799.
22. Lotjonen J, Kivisto S, Koikkalainen J, Smutek D, Lauerma K. Statistical shape model of atria, ventricles and epicardium from short- and long-axis MR images. Med Image Anal 2004;8:371–386.
23. Perperidis D, Mohiaddin R, Rueckert D. Construction of a 4D statistical atlas of the cardiac anatomy and its use in classification. Med Image Comput Comput Assist Interv Int Conf Med Image Comput Comput Assist Interv 2005;8:402–410.
24. Cerqueira MD, Weissman NJ, Dilsizian V, et al. Standardized myocardial segmentation and nomenclature for tomographic imaging of the heart: a statement for healthcare professionals from the Cardiac Imaging Committee of the Council on Clinical Cardiology of the American Heart Association. Circulation 2002;105:539–542.
25. Willcoxon F. Individual comparison by ranking methods. Biometrics 1945;1:80–83.
26. Fisher RA. On the interpretation of χ^2 from contingency tables, and the calculation of P. J R Stat Soc 1922;85:87–94.
27. Mestroni L, Maisch B, McKenna WJ, et al. Guidelines for the study of familial dilated cardiomyopathies. Eur Heart J 1999;20:93–102.
28. Mahon NG, Murphy RT, MacRae CA, Caforio AL, Elliott PM, McKenna WJ. Echocardiographic evaluation in asymptomatic relatives of patients with dilated cardiomyopathy reveals preclinical disease. Ann Intern Med 2005;143:108–115.
29. Henry WL, Gardin JM, Ware JH. Echocardiographic measurements in normal subjects from infancy to old age. Circulation 1980;62:1054–1061.
30. Young AA, Dokos S, Powell KA, et al. Regional heterogeneity of function in nonischemic dilated cardiomyopathy. Cardiovasc Res 2001;49:308–318.
31. McCrohon JA, Moon JC, Prasad SK, et al. Differentiation of heart failure related to dilated cardiomyopathy and coronary artery disease using gadolinium-enhanced cardiovascular magnetic resonance. Circulation 2003;108:54–59.